J Solid State Electrochem (2007) 11:763–772
DOI 10.1007/s10008-006-0219-7

ORIGINAL PAPER

Nonlinear magneto-optical effects and photomagnetism of electrochemically synthesized molecule-based magnets

Tomohiro Nuida · Toshiya Hozumi · Hiroko Tokoro · Kazuhito Hashimoto · Shin-ichi Ohkoshi

Received: 21 July 2006 / Accepted: 1 September 2006 / Published online: 21 November 2006

Abstract This article describes novel optical functionalities such as photomagnetic effects and magnetization-induced second harmonic generation (MSHG) in several cyano-bridged metal assemblies. Single crystal- and film-types of a cyano-bridged Cu–Mo bimetallic assembly, $Cs^{I}_{2}Cu^{II}_{7}\left[Mo^{IV}(CN)_8\right]_4 \cdot 6H_2O$, were electrochemically prepared. When this compound was irradiated with light, spontaneous magnetization with a Curie temperature (T_C) of 23 K was observed. Electrochemically prepared $Fe^{II}[Cr^{III}(CN)_6]_{2/3}\cdot 5H_2O$ thin film, which was a ferromagnet with T_C=21 K, showed photoreduced magnetization. This photomagnetism is due to the change of ferromagnetic coupling between Fe^{II} and Cr^{III}. MSHG was observed in $Cs^{I}Co^{II}[Cr^{III}(CN)_6]\cdot 0.5H_2O$. This $F\bar{4}3m$-type Prussian blue analog-based magnet is proven to be a piezoelectric ferromagnet, i.e., condensed matter with both piezoelectric and ferromagnetism. This MSHG is due to the coupling between a piezoelectric structure of $F\bar{4}3m$ and ferromagnetism with a T_C of 46 K.

Keywords Prussian blue analog · Cyano-bridged metal assembly · Photomagnetism · Nonlinear magneto-optics

Contribution to special issue “Magnetic field effects in Electrochemistry”.

T. Nuida · T. Hozumi · H. Tokoro · S. Ohkoshi (✉)
Department of Chemistry, School of Science,
The University of Tokyo,
7-3-1 Hongo,
Bunkyo-ku, Tokyo 113-0033, Japan
e-mail: ohkoshi@chem.s.u-tokyo.ac.jp

T. Nuida · H. Tokoro · K. Hashimoto · S. Ohkoshi
Department of Applied Chemistry, School of Engineering,
The University of Tokyo,
7-3-1 Hongo,
Bunkyo-ku, Tokyo 113-8656, Japan

H. Tokoro
Department of Physics, School of Science,
The University of Tokyo,
7-3-1 Hongo,
Bunkyo-ku, Tokyo 113-0033, Japan

Introduction

Prussian blue shows a blue color and is used as a dyeing material. Moreover, the electrochromic phenomenon of Prussian blue film has been studied in the field of electrochemistry [1]. The magnetic property of Prussian blue has also drawn much attention, and various interesting magnetic properties have been reported with its analogs [2–5]. In addition to Prussian blue analogs composed of hexacyanometalates $\left[M(CN)_6\right]^{n-}(M = Fe, Cr, Mn, \ldots)$, octacyanometalates $\left[M(CN)_8\right]^{n-}(M = Mo, W, \ldots)$ are also useful building blocks for functionalized molecule-based magnets because they can adopt three different spatial configurations [e.g., square antiprism (D_{4h}), dodecahedron (D_{2d}), and bicapped trigonal prism (C_{2v})] [6–29]. These cyano-bridged metal assemblies have been studied as functionalized molecule-based magnets [30–35]. In this review, we show the photomagnetic effect and nonlinear magneto-optical effect of the cyano-bridged metal assemblies synthesized by an electrochemical method.

Photomagnetism in copper–molybdenum polycyanide

A single crystal of $Cs^{I}_{2}Cu^{II}_{7}\left[Mo^{IV}(CN)_8\right]_4 \cdot 6H_2O$ was electrochemically prepared on Pt wire electrode. This

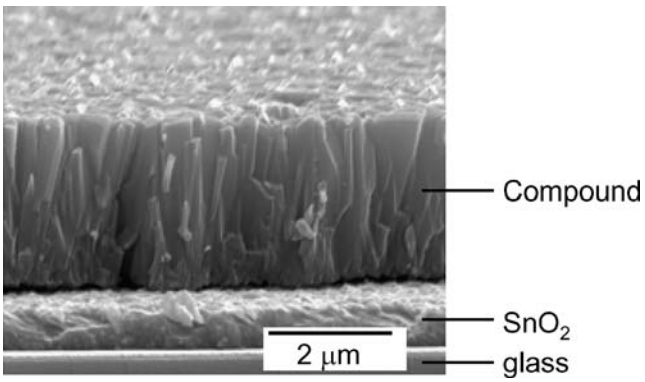

Fig. 1 SEM image of electrochemically synthesized $Cs^{I}_{2}Cu^{II}_{7}[Mo^{IV}(CN)_8]_4 \cdot 6H_2O$ film

compound was also prepared as a film on SnO_2-coated glass in the same electrochemical manner. When the sample, which shows paramagnetism due to Cu^{II} (S=1/2), was irradiated with light at 5 K, spontaneous magnetization with a T_C of 23 K was observed [36].

Electrochemical synthesis and crystal structure

The target material of $Cs^{I}_{2}Cu^{II}_{7}[Mo^{IV}(CN)_8]_4 \cdot 6H_2O$ was electrochemically prepared by reducing a mixed aqueous solution of $Cu^{II}(NO_3)_2 \cdot 3H_2O$ and $Cs_3[Mo^{V}(CN)_8] \cdot 2H_2O$ [37] in a standard three-electrode cell at a constant potential condition of +500 mV vs Ag/AgCl electrode. The electrolytic aqueous solutions were adjusted to pH=3 with HNO_3. After 3 days, dark purple single crystals that were 70±30 μm were obtained on Pt wire electrode. Elemental analyses confirmed that the formula was $Cs^{I}_{2}Cu^{II}_{7}[Mo^{IV}(CN)_8]_4 \cdot 6H_2O$. A film type of material was prepared on SnO_2-coated glass (Fig. 1). Elemental analyses showed that the formula of the film was consistent with that of the single crystal.

The electrochemical growth of the present compound is caused by the reduction of $[Mo^{v}(CN)_8]^{3-}$. Because the redox potential of $[Mo^{IV/V}(CN)_8]^{4-/3-}$ is +580 mV vs Ag/AgCl electrode, $[Mo^{v}(CN)_8]^{3-}$ is reduced to $[Mo^{IV}(CN)_8]^{4-}$ on the surface of the working electrode at a constant potential of +500 mV. Then, the produced $[Mo^{IV}(CN)_8]^{4-}$ reacts with Cu^{2+} ions, which results in the crystal of cyano-bridged Cu^{II}–Mo^{IV} complex being deposited on the electrode, as described by the following electrochemical reactions.

$$[Mo^{V}(CN)_8]^{3-} + e^{-} \rightarrow [Mo^{IV}(CN)_8]^{4-} \quad (1)$$

$$4[Mo^{IV}(CN)_8]^{4-} + 7Cu^{2+} + 2Cs^{+} \rightarrow Cs^{I}_{2}Cu^{II}_{7}[Mo^{IV}(CN)_8]_4 \cdot 6H_2O \quad (2)$$

X-ray single crystal structural analysis shows that this compound consists of a three-dimensional cyano-bridged Cu–Mo bimetallic assembly with a tetragonal structure of $I4/mmm$ space group [$a=b$=7.2444(9) Å, c=28.417(5) Å]. Figure 2a shows the coordination environments around Mo and Cu ions. This crystal has one coordination geometry for the Mo ions and two coordination geometries for the Cu ions (Cu1 and Cu2). A Mo ion links five Cu1 ions and three Cu2 ions through CN ligands. The coordination geometry of MoC_8 adopts a bicapped trigonal prism geometry. The Cu1 ion is coordinated to five cyanonitrogens and its geometry is square pyramidal. The Cu2 ion is

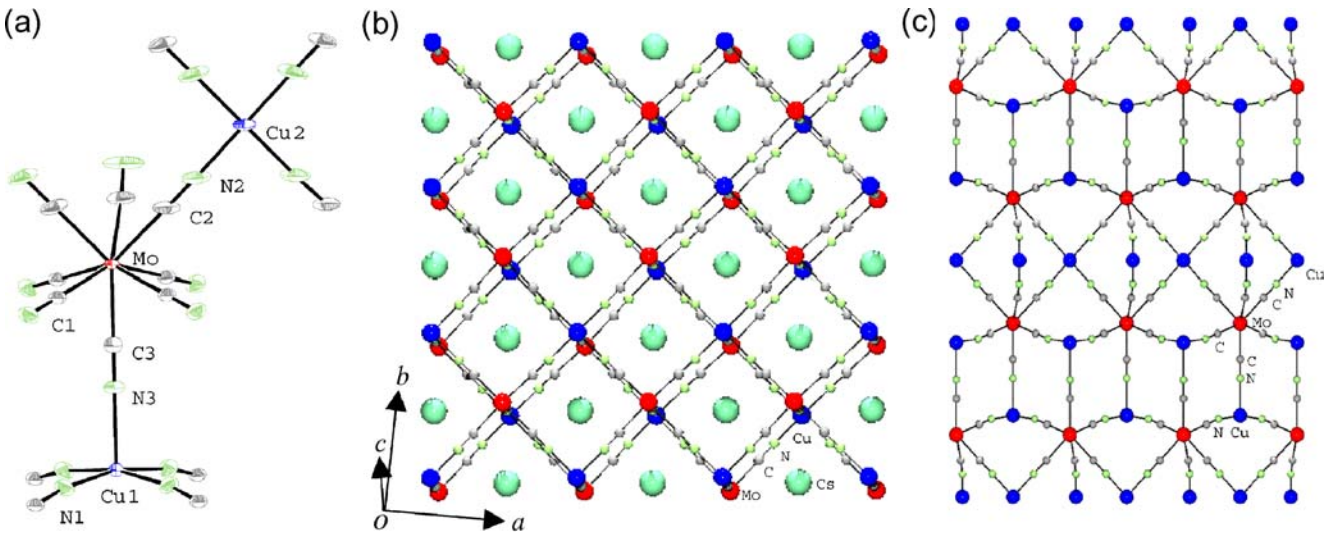

Fig. 2 Schematic illustration of the crystal structure of $Cs^{I}_{2}Cu^{II}_{7}[Mo^{IV}(CN)_8]_4 \cdot 6H_2O$: **a** ORTEP drawing of the coordination environments around Cu and Mo. Displacement ellipsoids are drawn at a 50% probability level. Cu2, C2, and N2 atoms are disordered and only selected atoms are drawn for clarity. **b** Structure of cyano-bridged $\{Cu[Mo(CN)_5]\}_n$ double layer. The occupancy of cesium atom is 50%. **c** Projection of three-dimensional network viewed towards the b axis. Water molecules and cesium atoms are omitted for clarity

coordinated to four cyanonitrogens and it has a square planar geometry. As shown in Fig. 2b, Cu1 and Mo form the square-grid layer through the cyanides in the *ab* plane, and the axial cyanide of $Cu1(NC)_5$ connects the upper (or lower) grid layer, which forms a double-layer structure. The cesium ion occupies the cubic cavity of this double layer with an occupancy of 1/2. Three out of the eight cyanides that surround the Mo ions stand out of the double layer and connect to Cu2 ions (Fig. 2c). There are eight symmetry equivalent positions of Cu2 on the plane of z=1/2. Thus, the occupancies of C2, N2, and Cu2 atoms are 3/8. Water molecules are present between the double layers as zeolitic water molecules.

Spectroscopic and magnetic properties

Figure 3 shows a UV-visible absorption spectrum of the prepared film. This compound possessed absorption bands near 520 and 650 nm. The absorption at 650 nm is assigned to a d–d transition of Cu^{II} ($^2B_1 \rightarrow {}^2B_2$ in square pyramidal Cu1 and/or $^2B_{1g} \rightarrow {}^2A_{1g}$ in square planar Cu2). In the light of previous papers [22, 25, 38], the other absorption at 520 nm is assigned to an intervalence transfer (IT) band between Mo^{IV}–CN–Cu^{II} and Mo^{V}–CN–Cu^{I}.

The electron spin resonance (ESR) spectra of the film at room temperature showed one dispersive peak with a g value of 2.14, which is probably due to paramagnetic Cu^{II} (S=1/2). Figure 4 shows the temperature dependence of the molar magnetic susceptibility (χ_M) in the field of 5,000 G. The $\chi_M T$ value at 300 K was equal to 3.1 $cm^3\ mol^{-1}$ K, which almost corresponds to the expected spin-only moment value of 3.0 $cm^3\ mol^{-1}$ K for S=1/2 and g_{Cu}= 2.14. As the temperature decreased, the $\chi_M T$ value was almost constant until 10 K, and then it decreased. The observed χ_M values obey the Curie–Weiss law, i.e., $\chi_M = C/(T-\theta)$, in the range of 10–300 K with a Weiss constant (θ) of −0.42 K and a Curie constant (C) of 3.13 $cm^3\ mol^{-1}$ K. The negative sign of the θ value suggests that the magnetic interaction between the Cu^{II} through the diamagnetic –NC–Mo^{IV}(S=0)–CN– bridge is a weak antiferromagnetic coupling.

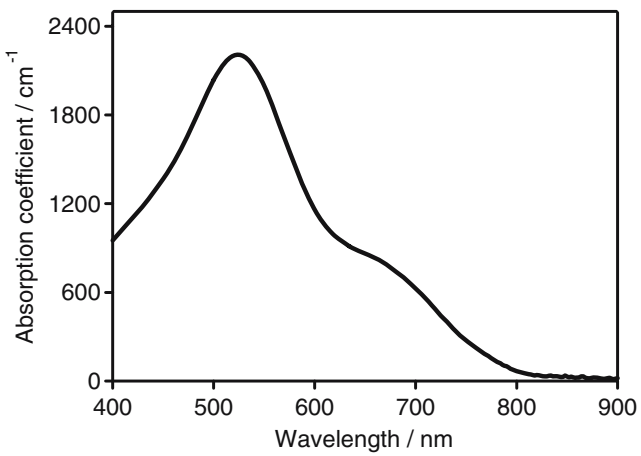

Fig. 3 UV-visible absorption spectrum of an electrochemically synthesized $Cs_2^{I}Cu_7^{II}[Mo^{IV}(CN)_8]_4 \cdot 6H_2O$ film

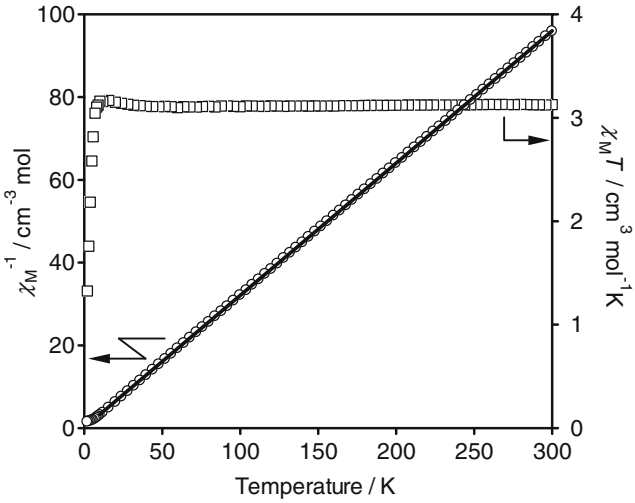

Fig. 4 Temperature dependence of the magnetic susceptibility measured under an external magnetic field of 5,000 G, $\chi_M T$ vs temperature plots and $\chi_M{}^{-1}$ vs temperature plots of $Cs_2^{I}Cu_7^{II}[Mo^{IV}(CN)_8]_4 \cdot 6H_2O$. The *solid line* represents the fitting line using Curie–Weiss law

Photomagnetic properties

When the sample was irradiated with blue light between 450 and 500 nm (5 mW/cm^2) at 5 K, a spontaneous magnetization with a T_C of 23 K and a magnetic hysteresis loop with a coercive field of 350 G were observed (Fig. 5). Warming the sample to 200 K returned the magnetic properties to the initial state. This photomagnetic behavior was repeatedly observed, indicating that the magnetization can be induced by a photon mode and recovered by a thermal mode.

To understand the mechanism of this photomagnetic behavior, infrared (IR) and ESR spectra after irradiating were measured. Figure 6 shows IR spectra when irradiating with blue light at 3 K. Irradiating decreased the IR peak due to Mo^{IV}–CN–Cu^{II}, and when the sample was warmed above 300 K and cooled to 3 K, the IR spectra was identical to the spectra before irradiating. Irradiating with 473-nm light at 103 K decreased the ESR peak due to Cu^{II}, as shown in Fig. 7. The signal intensity returned to the initial value after a thermal treatment of 300 K. These results indicate that irradiating decreases Mo^{IV} and Cu^{II}.

The photoinduced magnetization of this compound can be explained by the following mechanism (Fig. 8). The

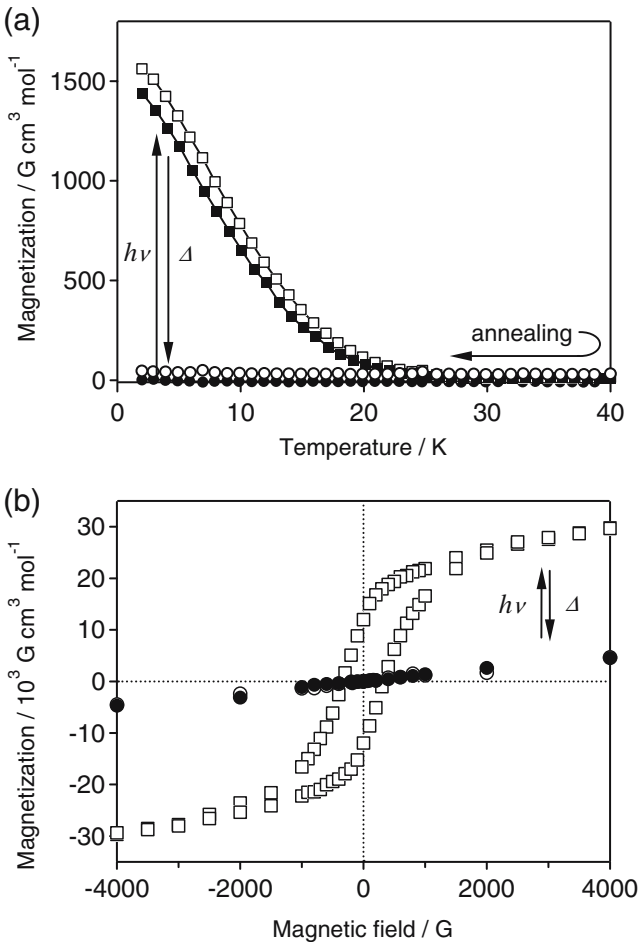

Fig. 5 Photomagnetic properties of $Cs_2Cu_7[Mo(CN)_8]_4{\cdot}6H_2O$: **a** magnetization vs temperature curves in a magnetic field of 10 G before light irradiation (*black circles*), after light irradiation (*white squares*), and after thermal treatment of 200 K (*white circles*). Remanent magnetization (*black squares*) of the irradiated sample was measured with increasing temperature after the temperature decreased at 10 G. **b** Magnetic hysteresis loops at 2 K before light irradiation (*black circles*), after light irradiation (*white squares*), and after thermal treatment of 200 K (*white circles*)

compound in the initial state is paramagnetic. Irradiating excites the compound to a charge transfer state. The compound in the excited state immediately relaxes to the initial state or forms the mixed-valence isomer (Mo^V–CN–Cu^I). In the present system, the decrease of Mo^{IV} and Cu^{II} indicates that the change from Mo^{IV}–CN–Cu^{II} to Mo^V–CN–Cu^I occurs. In this valence isomer state, the Mo^V ($4d^1$, S=1/2) has an unpaired electron, but Cu^I ($3d^{10}$, S=0) does not have an unpaired electron. However, 3/7 of the copper ions should remain as Cu^{II} due to the stoichiometric limitation in the present compound. The produced Mo^V is coordinated to 3.42 (=8×3/7) of Cu^{II} after the electron transfer is accomplished. A spontaneous magnetization appears due to the ferromagnetic coupling between the unpaired electrons on the Mo^V (S=1/2) and those on the Cu^{II} (S=1/2) of the irradiated compound.

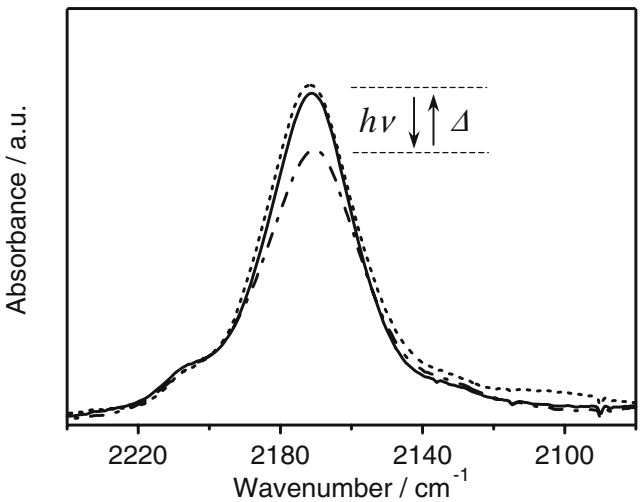

Fig. 6 IR spectra at 3 K before light irradiation (*solid line*), after light irradiation (*dash-dotted line*), and after thermal treatment of 300 K (*dotted line*) of $Cs_2Cu_7[Mo(CN)_8]_4{\cdot}6H_2O$

To investigate the structural changes, the X-ray powder diffraction (XRD) pattern with the light irradiation was also measured. Irradiating with blue light at 15 K, the lattice constant of the *a* (=*b*) axis increased, while that of the *c* axis remained the same. When the irradiated sample was warmed above 300 K and then cooled to 15 K, the XRD pattern returned to the initial pattern. This anisotropic structure expansion when irradiating suggests that the electron transfer from Mo^{IV} to square pyramidal Cu^{II} (Cu1) is dominant in this photoreaction because (1) the equatorial bond distance in square pyramidal Cu^{II} should be elongated when Cu^{II} is reduced to Cu^I (Fig. 9) [39] and (2)

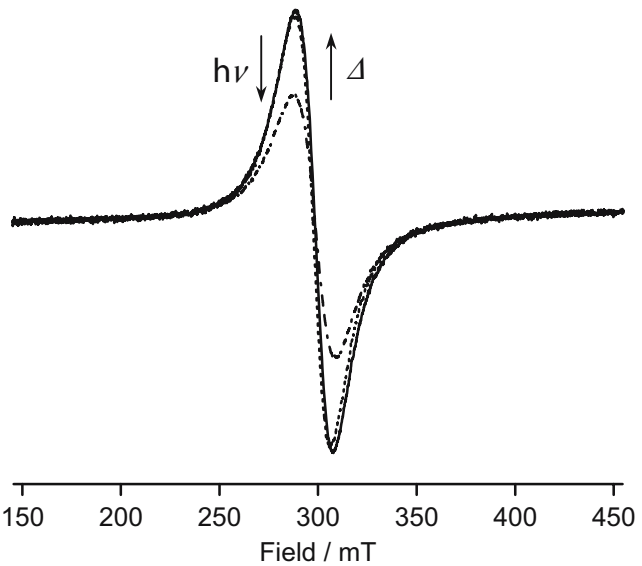

Fig. 7 ESR spectra at 103 K before light irradiation of 473 nm (*solid line*), after light irradiation (*dash-dotted line*), and after thermal treatment of 300 K (*dotted line*)

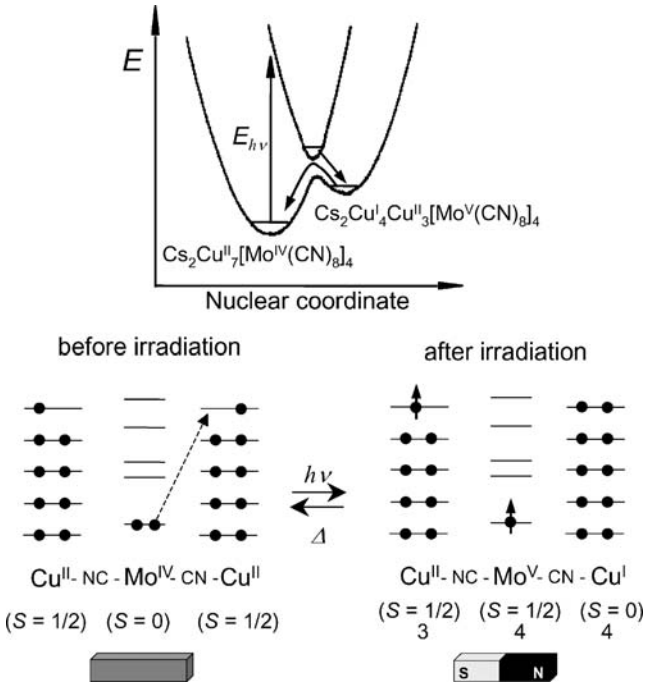

Fig. 8 Reaction scheme of photomagnetism of $Cs_2Cu_7[Mo(CN)_8]_4{\cdot}6H_2O$

square planar Cu^{I} is unstable and cannot exist even if square planar Cu^{II} (Cu2) accepts an electron from Mo^{IV}.

Photomagnetism in iron–chromium polycyanides

The magnetic properties and photomagnetic effects of the electrochemically prepared metal polycyanide film, $Fe^{II}[Cr^{III}(CN)_6]_{2/3}{\cdot}5H_2O$, were investigated. Magnetization measurements showed that it was a ferromagnet (parallel spin ordering) having a T_C=21 K. The spontaneous magnetization decreased optically by the photoexcitation of the IT band between Fe^{II} and Cr^{III}. This optically reduced magnetization persisted for a period of several days at 5 K after turning off the light [40, 41].

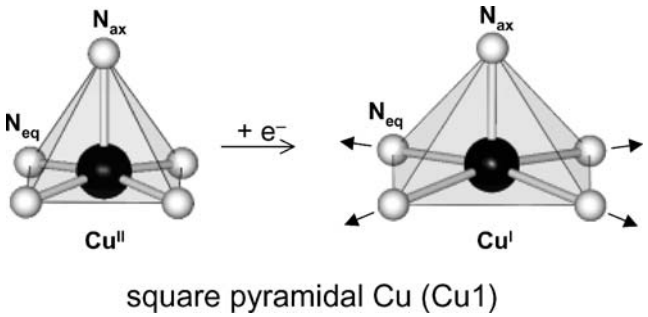

Fig. 9 Schematic illustration of the change in bond distances for five-coordinated square pyramidal Cu1 by the reduction from Cu^{II} to Cu^{I} in $Cs_2Cu_7[Mo(CN)_8]_4{\cdot}6H_2O$

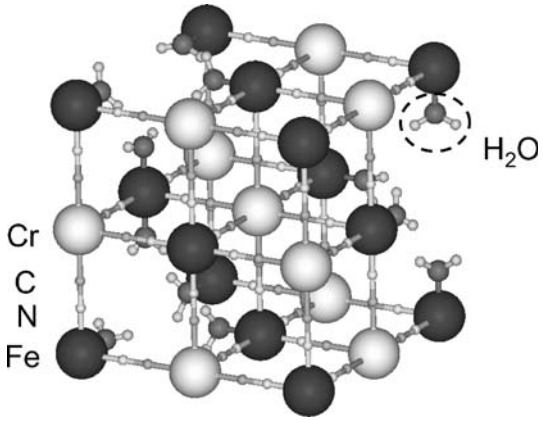

Fig. 10 Schematic structure of $Fe^{II}[Cr^{III}(CN)_6]_{2/3}{\cdot}5H_2O$. Zeolitic water molecules in the unit cell are omitted for clarity

Electrochemical synthesis and physical properties

The $Fe^{II}[Cr^{III}(CN)_6]_{2/3}{\cdot}5H_2O$ magnetic thin films were obtained on SnO_2-coated glass by reducing an aqueous solution containing $K_3[Cr(CN)_6]$ and $FeCl_3$ at −0.1 to −1.0 V vs saturated calomel electrode (SCE). The XRD pattern was consistent with that of a face-centered cubic (fcc) structure, with a lattice constant of 10.64 Å (Fig. 10). Figure 11 shows the current–voltammetric curve of the film obtained at −0.5 V vs SCE. The reduction peak was observed at −1.15 V vs SCE, and the film color was changed from brown to dark blue. This potential is equal to the reduction potential of $K_3[Cr^{III}(CN)_6]$, indicating that the Cr^{II}–CN moiety is formed in the iron–chromium polycyanide. The reoxidation peak was observed at −1.02 V vs SCE during the backscan, accompanied with the reverse color change. The field-cooled magnetization vs temperature plots of the prepared $Fe^{II}[Cr^{III}(CN)_6]_{2/3}{\cdot}5H_2O$ in an external magnetic field of 10 G showed an abrupt break at

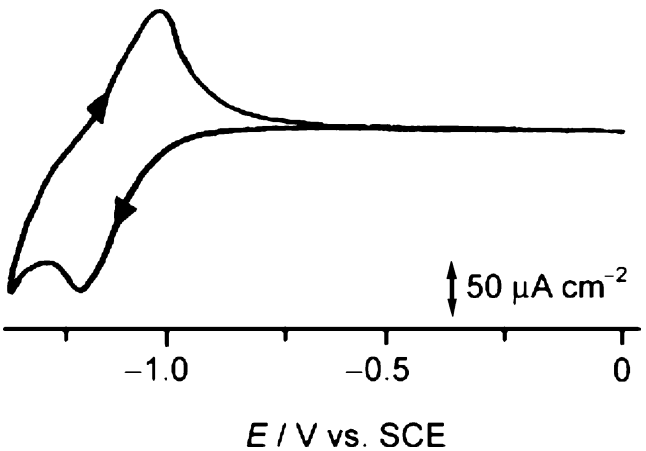

Fig. 11 Cyclic voltammogram for a $Fe[Cr(CN)_6]_{2/3}{\cdot}5H_2O$ film on SnO_2-coated glass (scan rate=50 mV s^{-1})

T_C=21 K (Fig. 12a). The coercive field was 200 G at 5 K. Figure 12b shows the magnetization vs the external magnetic field plots, indicating that the saturation magnetization value was 4.8 μ_B per $Fe^{II}[Cr^{III}(CN)_6]_{2/3}\cdot 5H_2O$. This result suggests that the magnetic coupling between Fe^{II} and Cr^{III} is possibly ferromagnetic. Let us consider the mechanism of the ferromagnetic coupling among spins in a $Fe^{II}[Cr^{III}(CN)_6]_{2/3}\cdot 5H_2O$ system. For typical Prussian blue analogs, their magnetic spin couplings are explained by a superexchange interaction [42–54]. Their fcc structures allow us to understand easily whether the superexchange interaction among transition metal ions is ferromagnetic or antiferromagnetic. For example, when the magnetic orbital symmetries of the metal ions through a cyano ligand are the same, the superexchange interaction is antiferromagnetic (J_{AF}). Conversely, when their magnetic orbital symmetries are different, the superexchange interaction is ferromagnetic (J_F). Usually, the J_{AF} contributes to spin alignment more effectively than the J_F [45, 50]. For the

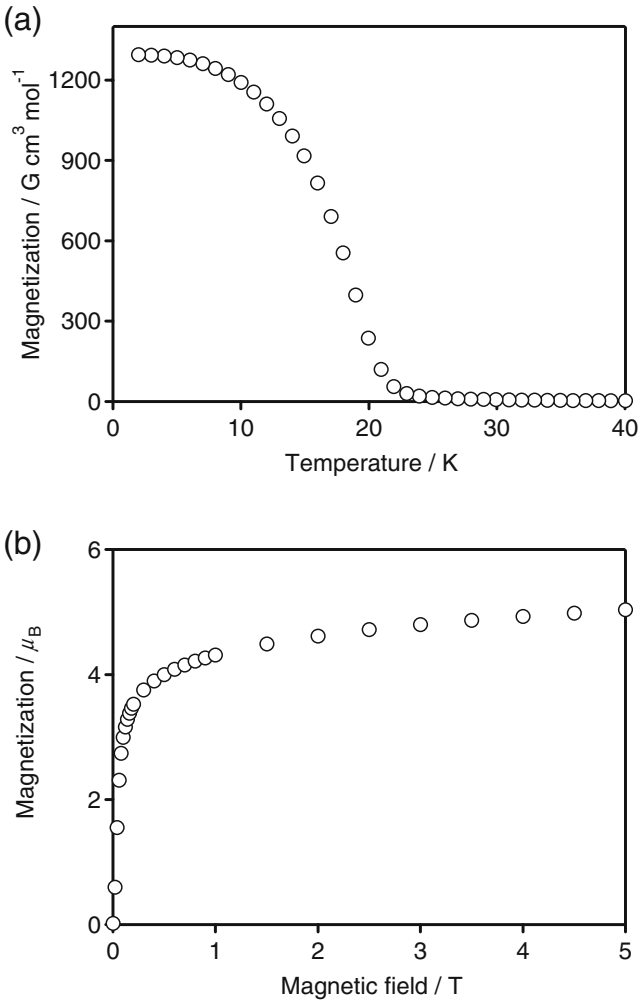

Fig. 12 Magnetic properties of $Fe^{II}[Cr^{III}(CN)_6]_{2/3}\cdot 5H_2O$: **a** field-cooled magnetization curve in a magnetic field of 10 G. **b** Magnetization vs external magnetic field curve at 5 K

$Fe^{II}[Cr^{III}(CN)_6]_{2/3}$ system, therefore, the magnetic interaction between Cr^{III} (t_{2g}^3, S=3/2) and Fe^{II} ($t_{2g}^4e_g^2$, S=2) is expected to be antiferromagnetic, suggesting that the compound should be a ferrimagnet. However, the experimental data suggest the opposite results. We have, therefore, to consider the other types of magnetic interactions. We are now considering the partial delocalization model as one of the possible explanations because this compound showed the IT band with an absorption maximum at 450 nm, which is characteristic of mixed-valence compounds [55–60].

Photomagnetic properties

With excitation of the IT band in the SQUID equipment at 5 K by 360–450 nm light, its magnetization value decreased gradually. For example, ca. 10% of magnetization was decreased in the external magnetic field of 10 G (Fig. 13). The reduced magnetization persisted for a period of several days at 5 K after turning off the light. The magnetic property of this irradiated compound returned to the initial state when the temperature was raised above 40 K and then the magnetization was measured at 5 K. The electronic states of the $Fe[Cr(CN)_6]_{2/3}\cdot 5H_2O$ before and after the irradiation were investigated by measuring the ^{57}Fe Mössbauer spectrum. To enhance the ^{57}Fe Mössbauer spectra, the sample was enriched with ^{57}Fe. As shown in Fig. 14a, the Mössbauer spectrum above T_C (at 77 K) before the irradiation was composed of two species. The outside peaks were a quadrupole split pair. The inner peaks constituted another quadrupole split pair. Both of these quadruploe pairs can be assigned to the high-spin

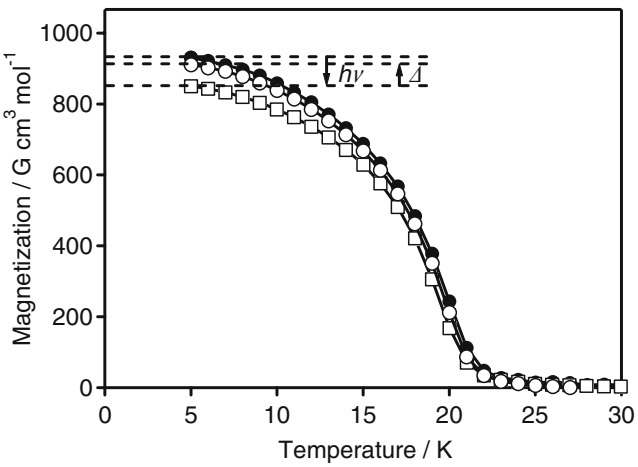

Fig. 13 Magnetization vs temperature curves of $Fe[Cr(CN)_6]_{2/3}\cdot 5H_2O$ in a magnetic field of 10 G before (*black circles*) and after (*white squares*) light irradiation. The curves before and after the irradiation are field-cooling and field-heating magnetization curves, respectively. Magnetic measurement sequence; 30 K→(*black circles*)→5 K (light irradiation)→(*white squares*)→30 K→80 K→(thermal treatment)→30 K→(*white circles*)→5 K

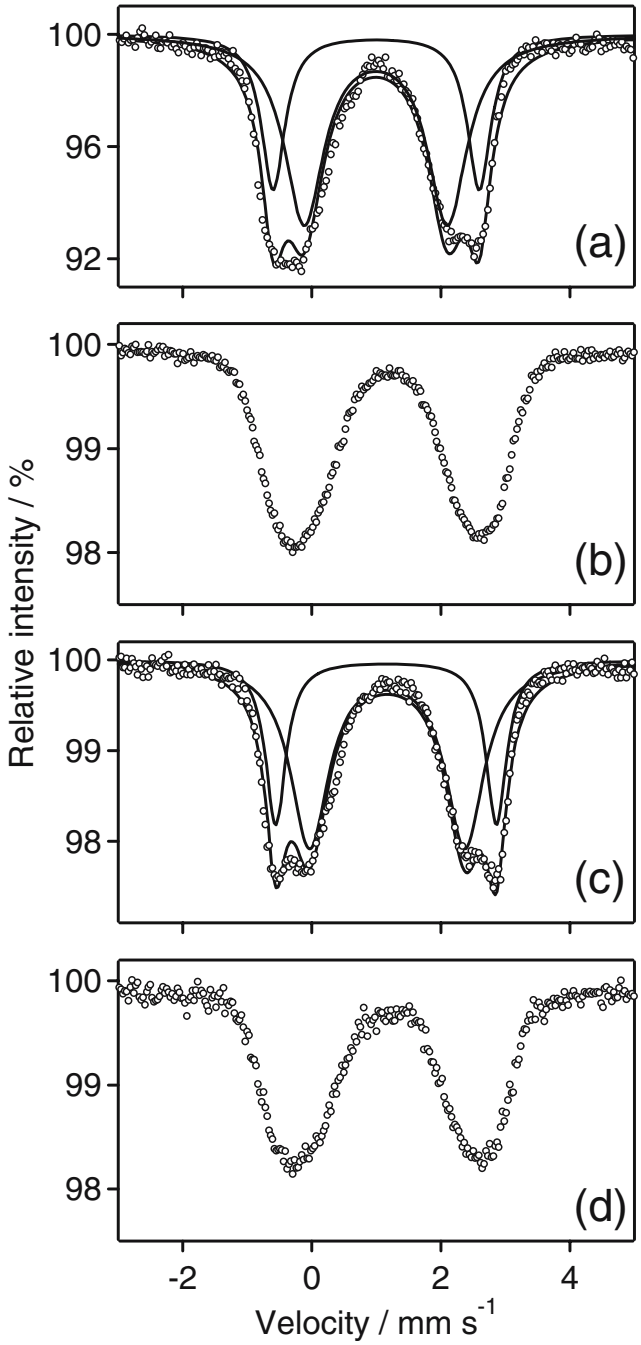

Fig. 14 ^{57}Fe Mössbauer spectra of $Fe[Cr(CN)_6]_{2/3}\cdot 5H_2O$: **a** at 77 K before the irradiation. **b** At 11 K before the irradiation. **c** At 11 K after the irradiation. **d** At 11 K after annealing (11→270→11 K)

Fe^{II} ($t_{2g}^4e_g^2$) [61, 62]. Below T_C (at 11 K), these two pairs changed to one broad pair (Fig. 14b), which can be explained by the spin ordering of Fe^{II} and Cr^{III}. After irradiation at 11 K, the spectrum changed to Fig. 14c, in which two split pairs appeared even below T_C. These two quadrupole pairs are again assigned to high-spin Fe^{II} ($t_{2g}^4e_g^2$), i.e., both the outside and the inner peaks were quadrupole split pairs. These results indicate that the spin state of iron is not changed by the irradiation and that neither electron transfer nor spin transition occurs photochemically. Conversely, the spectral pattern and line widths of the peaks after the irradiation were similar to those observed at 77 K before the irradiation, indicating that spins of Fe^{II} and Cr^{III} are not aligned after the irradiation anymore. These results suggest that a ferromagnetic state turned to a paramagnetic state without changing the valences of the metal ions. In other words, only the strength of the ferromagnetic coupling between Fe^{II} and Cr^{III} was disconnected by the irradiation. When the sample temperature was raised to 270 K and cooled to 11 K again, the spectrum returned to the one before the irradiation, as shown in Fig. 14d. The photoinduced magnetization decrease will be explained as follows: The photoexcited state is the mixed valence state of Cr^{III}–CN–Fe^{II} and Cr^{II}–CN–Fe^{III}. This photoexcited state would relax to a metastable state in which the ferromagnetic interaction is too weak to maintain the spins' ordering (Fig. 15). This metastable state returns to the original ferromagnetic state above 40 K.

We showed that magnetic coupling between Fe^{II} and Cr^{III} of the electrochemically prepared $Fe^{II}[Cr^{III}(CN)_6]_{2/3}\cdot 5H_2O$ is ferromagnetic. The magnetization of this compound was reduced in a photon mode by exciting the IT band. The spin state of iron (Fe^{II}, $t_{2g}^4e_g^2$, high spin) is not changed by the irradiation, but the strength of ferromagnetic coupling between Fe^{II} and Cr^{III} is decreased, forming a paramagnetic state. This paramagentic state returns to the original ferromagnetic state above 40 K. Using the Fe–Cr system, we also reported the photoinduced magnetic pole inversion in a mixed ferro–ferrimagnet, $(Fe^{II}_{0.40}Mn^{II}_{0.60})[Cr^{III}(CN)_6]_{2/3}\cdot 5H_2O$ [40].

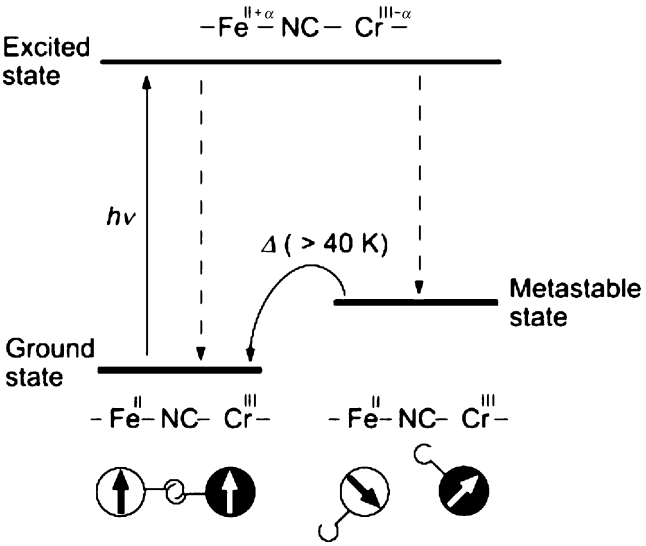

Fig. 15 Reaction scheme of photomagnetism of $Fe[Cr(CN)_6]_{2/3}\cdot 5H_2O$. *Arrows* show the direction of spins

Nonlinear magneto-optical effects in $F\bar{4}3m$-type cobalt–chromium polycyanide

The second harmonic generation (SHG) and magnetization-induced SHG (MSHG) of $Cs^{I}Co^{II}[Cr^{III}(CN)_6]\cdot 0.5H_2O$ were observed, and a large interaction between the nonlinear-optical response and magnetic spins was observed in this compound. This observation implies that $AM_A[M_B(CN)_6]$-type Prussian blue analogs are piezoelectric above T_C and piezoelectric ferromagnets below T_C.

$Cs^{I}Co^{II}[Cr^{III}(CN)_6]\cdot 0.5H_2O$ of the target sample was prepared by reacting a mixed aqueous solution of $K_3[Cr^{III}(CN)_6]$ and $Cs^{I}Cl$ with a mixed aqueous solution of $Co^{II}Cl_2$ and $Cs^{I}Cl$. $Co^{II}[Cr^{III}(CN)_6]_{2/3}\cdot 4.8H_2O$ of the reference sample was prepared by reacting an aqueous solution of $K_3[Cr^{III}(CN)_6]$ with an aqueous solution of $Co^{II}Cl_2$ [63]. SEM images showed that the prepared samples consisted of cubic microcrystals with particle sizes of 140±30 nm ($CsCo[Cr(CN)_6]\cdot 0.5H_2O$), 80±10 nm ($Co[Cr(CN)_6]_{2/3}\cdot 4.8H_2O$).

When $Cs^{I}Co^{II}[Cr^{III}(CN)_6]\cdot 0.5H_2O$ (Fig. 16) was irradiated by 1,064-nm light at 295 K, 532-nm light was observed. Because the intensity of the 532-nm light increased with the square of the incident light intensity (inset of Fig. 17a), the observed 532-nm light is clearly SH light. The temperature dependence of the SH intensity showed that the SH intensity was nearly constant between 295 and 55 K, but the SH intensity increased below 55 K, and the intensity at 5 K was 1.9 times larger than the intensity at 295 K (Fig. 17a). This temperature dependence corresponds to the temperature dependence of magnetization of this system (Co^{II}: S=3/2, Cr^{III}: S=3/2), which is a ferromagnet with a T_C of 46 K (Fig. 17b). In contrast, $Co^{II}[Cr^{III}(CN)_6]_{2/3}\cdot 4.8H_2O$, the reference sample, did not exhibit SHG over the entire temperature range.

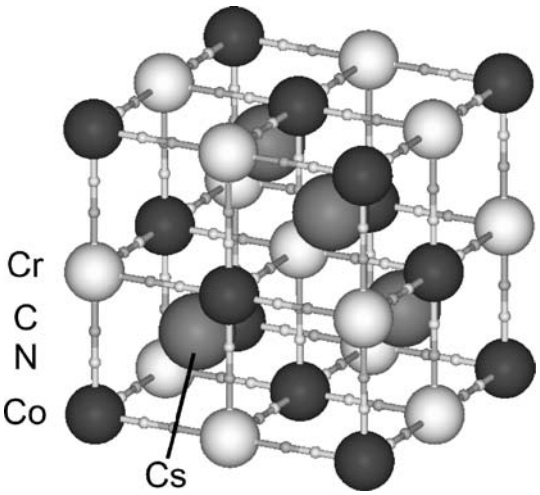

Fig. 16 The unit cell of $Cs^{I}Co^{II}[Cr^{III}(CN)_6]$ ($F\bar{4}3m$). Water molecules in the unit cell are omitted

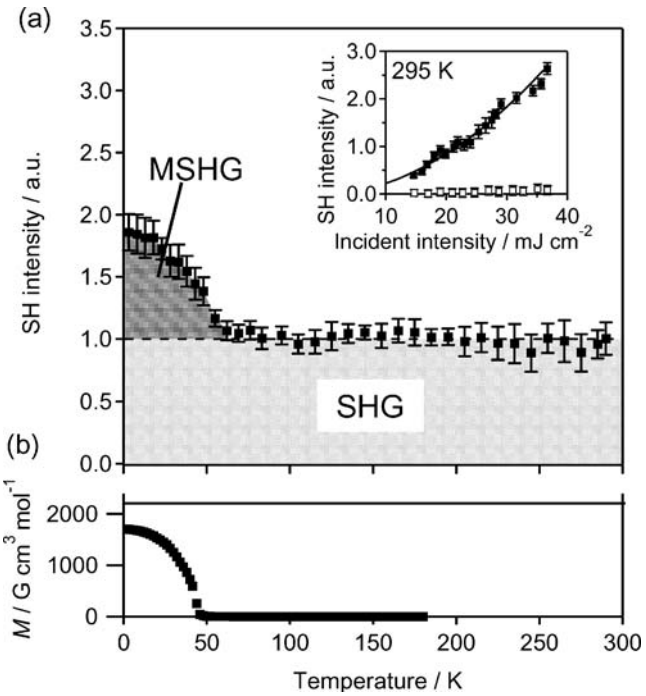

Fig. 17 **a** Temperature dependence of the SH intensity generated from $Cs^{I}Co^{II}[Cr^{III}(CN)_6]\cdot 0.5H_2O$. The *inset* shows SH intensity vs incident light intensity of $Cs^{I}Co^{II}[Cr^{III}(CN)_6]\cdot 0.5H_2O$ (*black squares*) and $Co[Cr(CN)_6]_{2/3}\cdot 4.8H_2O$ (*white squares*) at 295 K. The *solid line* represents the fitting curve using a quadratic function. **b** Field-cooled magnetization curve of $Cs^{I}Co^{II}[Cr^{III}(CN)_6]\cdot 0.5H_2O$ in a magnetic field of 10 G

The SHG observed in $Cs^{I}Co^{II}[Cr^{III}(CN)_6]\cdot 0.5H_2O$ is understood by the following: The second-order optical response is described by $P_i(2\omega)=\chi_{ijk}^{(2)}(-2\omega;\omega,\omega)E_j(\omega)E_k(\omega)$, where $P_i(2\omega)$ is the second-order nonlinear polarization and $\chi_{ijk}^{(2)}$ is the second-order nonlinear susceptibility tensor. The XRD patterns show that the crystal structures of $Cs^{I}Co^{II}[Cr^{III}(CN)_6]\cdot 0.5H_2O$ and $Co^{II}[Cr^{III}(CN)_6]_{2/3}\cdot 4.8H_2O$ are $F\bar{4}3m$ and $Fm\bar{3}m$, respectively. In $AM_A[M_B(CN)_6]$-type Prussian blue analogs, the M_A ions coordinate to six cyanonitrogen and the A ion is located in the interstitial site of the lattice (Fig. 16) [45, 64–66]. It is noteworthy that the position of the A ion in this type of crystal produces a $\bar{4}$ rotoinversion operator. The crystal structure is noncentrosymmetric, and hence, SHG is permitted in $Cs^{I}Co^{II}[Cr^{III}(CN)_6]\cdot 0.5H_2O$. This space group has a crystallographic term ($\chi_{ijk}^{(2)cry}$) in the second-order nonlinear susceptibility, i.e., $\chi_{xyz}^{(2)cry}$, $\chi_{yzx}^{(2)cry}$, $\chi_{zxy}^{(2)cry}$, and $\chi_{xyz}^{(2)cry}=\chi_{yzx}^{(2)cry}=\chi_{zxy}^{(2)cry}$. Furthermore, below T_C, the magnetic ordering creates a magnetic term ($\chi_{ijk}^{(2)mag}$). This second-order nonlinear susceptibility term is called the MSHG [67–73]. Thus, the enhanced SH intensity below T_C is due to the creation of the $\chi_{ijk}^{(2)mag}$ term. Because the ferromagnetic phase of $Cs^{I}Co^{II}[Cr^{III}(CN)_6]\cdot 0.5H_2O$ is in the $I\bar{4}\underline{m}2$ magnetic space group [74], the nonzero tensor elements in $\chi_{ijk}^{(2)}$ are described by the contribution

of the $\chi_{ijk}^{(2)cry}$ and $\chi_{ijk}^{(2)mag}$, i.e., $\chi_{xyz}^{(2)cry}+\chi_{xyz}^{(2)mag}$, $\chi_{yzx}^{(2)cry}+\chi_{yzx}^{(2)mag}$, $\chi_{zxy}^{(2)cry}+\chi_{zxy}^{(2)mag}$. In contrast, $Co^{II}[Cr^{III}(CN)_6]_{2/3}\cdot 4.8H_2O$ is a $Fm\bar{3}m$-type crystal and centrosymmetric. Thus, all tensor elements of $\chi_{ijk}^{(2)}$ are zero and SHG is forbidden.

SHG and MSHG were observed in $F\bar{4}3m$-type Prussian blue analogs; $Cs^{I}Co^{II}[Cr^{III}(CN)_6]\cdot 0.5H_2O$. These observations are remarkable results in the fields of magneto-optics and magnetic materials because reports of bulk MSHG have been limited [67, 70, 72, 73].[1] Because a variety of $F\bar{4}3m$-type Prussian blue analogs can be prepared, the studies of piezoelectric ferromagnets will get ahead with this series.

Conclusions

We have described photomagnetism in cyano-bridged metal assemblies. Single crystal- and film-types of $Cs^{I}_2Cu^{II}_7[Mo^{IV}(CN)_8]_4\cdot 6H_2O$ were electrochemically prepared. When the compound was irradiated with 450–500 nm light, a spontaneous magnetization with a T_C of 23 K was observed. In this photoinduced magnetization, ferromagnetic ordering between Mo^{V} (S=1/2) and Cu^{II} (S=1/2) was produced by exciting of the IT band between molybdenum and copper. With $Fe^{II}[Cr^{III}(CN)_6]_{2/3}\cdot 5H_2O$ thin film, the photomagnetic effect was investigated. The spontaneous magnetization decreased optically by the photoexcitation of the IT band between Fe^{II} and Cr^{III}. In this effect, the spin state of iron did not change, but the strength of a ferromagnetic interaction between Fe^{II} and Cr^{III} decreased after the irradiation, forming a paramagnetic metastable state. Furthermore, we have demonstrated an example that showed MSHG effect with $Cs^{I}Co^{II}[Cr^{III}(CN)_6]\cdot 0.5H_2O$. This indicates that a $F\bar{4}3m$-type Prussian blue analog-based magnet is proven to be a piezoelectric ferromagnet. These novel optical functionalities of cyano-bridged metal assemblies will open a new avenue in the study of many fields, such as electrochemistry, photochemistry, and magneto-optics.

Acknowledgements The present research is supported in part by a Grant-in-Aid for 21st Century Center of Excellence programs for Frontiers in Fundamental Chemistry, a Grant-in-Aid for Scientific Research from the Ministry of Education, Culture, Sports, Science, and Technology of Japan, and JSPS and RFBR under the Japan-Russia Research Cooperative Program.

[1] The present MSHG is essentially different from the MSHG observed in electrochemically synthesized $(Fe_xCr_{1-x})[Cr(CN)_6]_{2/3}\cdot 5H_2O$ films of references [72] and [73]. The latter is due to an electrochemically distorted crystal structure ($C2$ space group).

References

1. Itaya K, Uchida I, Neff VD (1986) Acc Chem Res 19:162
2. Verdaguer M, Bleuzen A, Marvaud V, Vaisserman J, Seuleiman M, Desplanches C, Scuiller A, Train C, Garde R, Gelly G, Lomenech C, Rosenman I, Veillet P, Cartier C, Villain F (1999) Coord Chem Rev 192:1023
3. Ohkoshi S, Hashimoto K (2001) J Photochem Photobiol C 2:71
4. Ohkoshi S, Hashimoto K (2002) Electrochem Soc Interface 11:34
5. Ohkoshi S, Tokoro H, Hashimoto K (2005) Coord Chem Rev 249:1830
6. Zhong ZJ, Seino H, Mizobe Y, Hidai M, Fujishima A, Ohkoshi S, Hashimoto K (2000) J Am Chem Soc 122:2952
7. Bonadio F, Gross M, Evans HS, Decurtins S (2002) Inorg Chem 41:5891
8. Rombaut G, Golhen S, Ouahab L, Mathonière C, Kahn O (2000) J Chem Soc Dalton Trans 3609
9. Li DF, Gao S, Zheng L, Tang W (2002) J Chem Soc Dalton Trans 2805
10. Li DF, Zheng LM, Zhang Y, Huang J, Gao S, Tang WX (2003) Inorg Chem 42:6123
11. Podgajny R, Korzeniak T, Balanda M, Wasiutynski T, Errington W, Kemp TJ, Alcock NW, Sieklucka B (2002) Chem Commun 1138
12. Ohkoshi S, Arimoto Y, Hozumi T, Seino H, Mizobe Y, Hashimoto K (2003) Chem Commun 2772
13. Hozumi T, Ohkoshi S, Arimoto Y, Seino H, Mizobe Y, Hashimoto K (2003) J Phys Chem B 107:11571
14. Li DF, Zheng LM, Wang XY, Huang J, Gao S, Tang WX (2003) Chem Mater 15:2094
15. Garde R, Desplanches C, Bleuzen A, Veillet P, Verdaguer M (1999) Mol Cryst Liq Cryst 334:587
16. Zhong ZJ, Seino H, Mizobe Y, Hidai M, Verdaguer M, Ohkoshi S, Hashimoto K (2000) Inorg Chem 39:5095
17. Li DF, Gao S, Zheng LM, Sun WY, Okamura T, Ueyama N, Tang WX (2002) New J Chem 26:485
18. Song Y, Ohkoshi S, Arimoto Y, Seino H, Mizobe Y, Hashimoto K (2003) Inorg Chem 42:1848
19. Herrera JM, Bleuzen A, Dromzée Y, Julve M, Lloret F, Verdaguer M (2003) Inorg Chem 42:7052
20. Kashiwagi T, Ohkoshi S, Seino H, Mizobe Y, Hashimoto K (2004) J Am Chem Soc 126:5024
21. Sra AK, Andruh M, Kahn O, Golhen S, Ouahab L, Yakhmi JV (1999) Angew Chem Int Ed Engl 38:2606
22. Ohkoshi S, Machida N, Zhong ZJ, Hashimoto K (2001) Synth Met 122:523
23. Ohkoshi S, Machida N, Abe Y, Zhong ZJ, Hashimoto K (2001) Chem Lett 312
24. Ohkoshi S, Tokoro H, Hozumi T, Zhang Y, Hashimoto K, Mathonière C, Bord I, Rombaut G, Verelst M, Cartier C, Villain F (2006) J Am Chem Soc 128:270
25. Rombaut G, Verelst M, Golhen S, Ouahab L, Mathonière C, Kahn O (2001) Inorg Chem 40:1151
26. Rombaut G, Mathonière C, Guionneau P, Golhen S, Ouahab L, Verelst M, Lecante P (2001) Inorg Chim Acta 326:27
27. Herrera JM, Marvaud V, Verdaguer M, Marrot J, Kalisz M, Mathonière C (2004) Angew Chem Int Ed Engl 43:5468
28. Bennett MV, Long JR (2003) J Am Chem Soc 125:2394
29. Ohkoshi S, Ikeda S, Hozumi T, Kashiwagi T, Hashimoto K (2006) J Am Chem Soc 128:5320
30. Miller JS, Epstein AJ (1994) Angew Chem Int Ed Engl 33:385
31. Kahn O (1993) Molecular magnetism. Wiley, New York
32. Gatteschi D, Kahn O, Miller JS, Palacio F (eds) (1991) Magnetic molecular materials. Kluwer, Dordrecht

33. Day P, Underhill AE (eds) (1999) Philos Trans R Soc Lond A 357:2851
34. Tamaki H, Zhong ZJ, Matsumoto N, Kida S, Koikawa M, Achiwa N, Hashimoto Y, Ōkawa H (1992) J Am Chem Soc 114:6974
35. Smith JA, Galán-Mascarós JR, Clérac R, Dunbar KR (2000) Chem Commun 1077
36. Hozumi T, Hashimoto K, Ohkoshi S (2005) J Am Chem Soc 127:3864
37. Bok LDC, Leipoldt JG, Basson SS (1975) Z Anorg Allg Chem 415:81
38. Hennig H, Rehorek A, Rehorek D, Thomas P (1984) Inorg Chim Acta 86:41
39. Holloway CE, Melnik M (1995) Rev Inorg Chem 15:147
40. Ohkoshi S, Yorozu S, Sato O, Iyoda T, Fujishima A, Hashimoto K (1997) Appl Phys Lett 70:1040
41. Ohkoshi S, Einaga Y, Fujishima A, Hashimoto K (1999) J Electroanal Chem 473:245
42. Hoden AN, Matthias BT, Anderson PW, Luis HW (1956) Phys Rev 102:1463
43. Griebler WD, Babel DZ (1982) Z Naturforsch T B 87:832
44. Mallah T, Thiebaut S, Verdaguer M, Veillet P (1993) Science 262:1554
45. Entley WR, Girolami GS (1994) Inorg Chem 33:5165
46. Ferlay S, Mallah T, Ouahés R, Veillet P, Verdaguer M (1995) Nature 378:701
47. William RE, Girolami GS (1995) Science 268:397
48. Sato O, Iyoda T, Fujishima A, Hashimoto K (1996) Science 271:49
49. Buschmann WE, Paulson SC, Wynn CM, Gïrtu MA, Epstein AJ, White AJ, Miller JS (1997) Adv Mater 9:645
50. Ohkoshi S, Sato O, Iyoda T, Fujishima A, Hashimoto K (1997) Inorg Chem 36:268
51. Ohkoshi S, Iyoda T, Fujishima A, Hashimoto K (1997) Phys Rev B 56:11642
52. Ohkoshi S, Fujishima A, Hashimoto K (1998) J Am Chem Soc 120:5349
53. Ohkoshi S, Abe Y, Fujishima A, Hashimoto K (1999) Phys Rev Lett 82:1285
54. Ohkoshi S, Arai K, Sato Y, Hashimoto K (2004) Nat Mater 3:857
55. Brown DB (1980) Mixed valence compounds (NATO ASI). Reidel, Dordrecht
56. Prassides K (1991) Mixed valency systems: applications in chemistry, physics and biology (NATO ASI). Kluwer, Dordrecht
57. Robin MB, Day P (1967) Adv Inorg Chem Radiochem 10:247
58. Hush NS (1967) Prog Inorg Chem 8:391
59. Piepho SB, Krausz ER, Schatrz PN (1978) J Am Chem Soc 100:2996
60. Wong KY, Schatz PN (1981) Prog Inorg Chem 28:369
61. Brown DB, Shriver DF, Schwartz LH (1968) Inorg Chem 7:77
62. Reguera E, Bertrán JF, Nuñez L (1994) Polyhedron 13:1619
63. Ohkoshi S, Hashimoto K (1999) Chem Phys Lett 314:210
64. Babel D (1986) Comments Inorg Chem 5:285
65. Verdaguer M, Bleuzen A, Train C, Garde R, Fabrizi de Biani F, Desplanches C (1999) Philos Trans R Soc Lond Ser A Math Phys Sci 357:2959
66. Ruiz E, Rodríguez-Fortea A, Alvarez S, Verdaguer M (2005) Chem Eur 11:2135
67. Aktsipetrov OA, Braginskii OV, Esikov A (1990) Sov J Quantum Electron 20:259
68. Reif J, Zink JC, Schneider CM, Kirschner J (1991) Phys Rev Lett 67:2878
69. Spierings G, Koutsos V, Wierenga HA, Prins MWJ, Abraham D, Rasing Th (1993) J Magn Magn Mater 121:109
70. Fiebig M, Fröhlich D, Krichevtsov BB, Pisarev RV (1994) Phys Rev Lett 73:2127
71. Rasing Th, Groot Koerkamp M, Koopmans B, van der Berg H (1996) J Appl Phys 79:6181
72. Ikeda K, Ohkoshi S, Hashimoto K (2001) Chem Phys Lett 349:371
73. Ohkoshi S, Shimura J, Ikeda K, Hashimoto K (2005) J Opt Soc Am B 22:196
74. Briss RR (1966) Symmetry and magnetism. North-Holand, Amsterdam